Available online at www.sciencedirect.com
ScienceDirect
Catalysis Today 119 (2007) 156–165
CATALYSIS TODAY
www.elsevier.com/locate/cattod

CH_4-SCR of NO over Co and Pd ferrierite catalysts: Effect of preparation on catalytic performance

A.P. Ferreira [a], S. Capela [b], P. Da Costa [c], C. Henriques [b,*], M.F. Ribeiro [b], F. Ramôa Ribeiro [b]

[a] *Instituto Superior de Ciências da Saúde, Egas Moniz, 2825 Monte da Caparica, Portugal*
[b] *Departamento de Engenharia Química, Instituto Superior Técnico, Av. Rovisco Pais, 1049-001 Lisboa, Portugal*
[c] *Université Pierre et Marie Curie, Laboratoire de Réactivité de Surface, 4, Place Jussieu, 75252 Paris, France*

Available online 18 September 2006

Abstract

Selective catalytic reduction of NO with methane (CH_4-SCR) in the presence of oxygen excess and water vapour was studied over two bimetallic cobalt/palladium-based FER catalysts, which differ on the order of introduction of metal ions. H_2-TPR and UV–vis analysis showed that the simple change in the order of addition of metals to catalyst, gives rise to totally diverse species (Co^{2+} ions, Co oxides, Co-oxo cations and Pd species) both in type and quantity but also in location within zeolite framework. Experiments of TPD and TPSR of NO and NO_2 provided important information to establish a relation between the various active sites formed on both catalysts and their function in the reaction mechanism. The importance of NO_2 in the mechanism of NO reaction with CH_4 and O_2 was explored and the catalyst with a higher capacity to retain adsorbed NO_2 is the less active for deNO_x. The preparation of a bimetallic catalyst active for NO reduction must provide the proximity between Co and Pd species, and the presence of Co-oxo cations together with palladium species seem to be essential. Furthermore, a suitable amount of cobalt oxides must exist in order to originate NO_2 that is the main reaction intermediate. Nevertheless, an excessive amount of these Co species can lead to an increase of adsorbed NO_2, which reduces the rate of the reaction of some of the mechanism steps.

Keywords: NO; CH_4-SCR; Co; Pd; FER zeolite; TPSR; TPD

1. Introduction

The selective catalytic reduction (SCR) of nitrogen oxides with methane is a promising technology to control NO_x emission from natural gas-based stationary sources. Cobalt-based zeolites have been reported to have good catalytic performances for CH_4-SCR of NO in the presence of oxygen excess [1,2]. Bimetallic zeolites, with cobalt and palladium, show an increase of activity and stability when compared with monometallic Co catalysts [3–8]. However, they still show a significant loss of activity and stability when water vapour is present in the reaction mixture. In general, catalytic activity is restored when water is suppressed from the gas stream, indicating a competitive adsorption in active sites, but it is a problem that still remains.

Understanding the reaction mechanism, the structure and function of catalyst active sites and structure–activity or selectivity relationships have been a matter of concern and intense research. Recent works on catalysis by transition metal-exchanged zeolites indicate that the specific activity of present species (isolated metal ions, clusters, oxides) greatly depend on their location inside the network of cavities or even in the external surface of zeolite crystallites [9]. An attempt to clarify the location of cations in the zeolite structure was made by Wichterlová et al. [10–12] who proposed for FER structure three types of bare Co^{2+} ions with different coordination, depending on the location in the available exchange sites α, β and γ. The α site is located in the main ferrierite channels and a cation in this site is coordinated with four oxygen atoms, creating a rectangle on the wall of the main channel. The β site corresponds to cobalt ions located in the plane of a deformed six-membered ring of the eight-ring channel and it is coordinated to six oxygen atoms. The γ site respects to the location in the eight-ring channels.

* Corresponding author. Tel.: +351 218417325; fax: +351 218419198.
E-mail address: pccarlos@alfa.ist.utl.pt (C. Henriques).

0920-5861/$ – see front matter © 2006 Elsevier B.V. All rights reserved.
doi:10.1016/j.cattod.2006.08.005

The reaction pathway of NO SCR with CH_4 is complex and several types of mechanisms have been suggested involving different catalytic functions [13–16] suggesting that an appropriate balance of the suitable catalytic sites should be a fundamental goal in order to obtain an active and stable catalyst.

The preparation method for the introduction of the metallic cations can lead to the formation of different active sites with different activities and stability, related for example with the location in the zeolite framework and with the ability of ions migration and sintering [4].

The present work consists on the study of the SCR of NO with methane in the presence of oxygen excess, using Pd and Co HFER bimetallic catalysts, whose preparation procedure differs on the metal introduction order. The establishment of a relation between the formed active species in each catalyst and their catalytic behaviour and function in the mechanism of the reaction will be attempted.

2. Experimental

2.1. Catalyst preparation

2.1.1. NH_4-FER form

An alkali form of ferrierite, NaK-FER, with a ratio of Si/Al = 9, was provided by TOSOH Co., Japan. The NH_4-FER form was prepared by ion-exchange at 80 °C for 3 h, three times, with a 4.0 M NH_4NO_3 solution, under strong agitation. After the exchange, the catalyst was washed with distilled water and dried at 100 °C for 12 h.

The catalysts prepared for this study were obtained by ion-exchanging NH_4-FER form with the required cations. The main difference concerning the preparation of the catalysts is related with the order of introduction of the metal. Two catalysts were prepared: (i) PdCo-HFER in which Co was introduced prior to Pd and (ii) CoPd-HFER with Pd as the first cation to be exchanged.

2.1.1.1. PdCo-HFER catalyst. The catalyst was prepared in two steps. Co-HFER was firstly obtained the by ion-exchanging the NH_4-FER form with a 0.032 M $Co(CH_3COO)_2$ (Fluka) solution and the ratio between the volume of solution and the catalyst mass (v/w) was 50. The ion-exchange occurs at 80 °C during 24 h, under a strong agitation. The catalyst was washed with distilled water and dried at 100 °C for 12 h. This procedure was followed by calcination at 500 °C (3 h) under air flow (4 L h^{-1} g^{-1}) with a heating rate of 5 °C min^{-1}. The second step concerns to Pd introduction by ion-exchanging Co-HFER catalyst with a solution of Pd. The palladium solution was prepared with the precise required amount of a solution of $Pd(NH_3)_4(NO_3)_2$ (Aldrich) to obtain 0.15 wt.% Pd. The palladium solution is diluted in the water volume calculated for a ratio v/w = 50. The exchange occurs at room temperature during 24 h under a strong agitation. The catalyst was washed with distilled water and dried at 100 °C for 12 h. Then it was calcined at 450 °C (8 h) under air flow (4 L h^{-1} g^{-1}) with a heating rate of 1 °C min^{-1}. The obtained catalyst was designated by PdCo-HFER.

2.1.1.2. CoPd-HFER catalyst. A Pd-HFER sample was prepared by ion-exchanging HFER form following the same procedure as reported previously for the introduction of Pd in a Co-HFER sample. CoPd-HFER was obtained by ion-exchanging the Pd-HFER catalyst, already calcined at 450 °C, with a 0.032 M $Co(CH_3COO)_2$ solution. The ion-exchange occurs at 80 °C during 24 h, under a strong agitation. The catalyst was washed with distilled water and dried at 100 °C for 12 h. Calcination was carried out at 450 °C (8 h) under air flow (4 L h^{-1} g^{-1}) with a heating rate of 1 °C min^{-1}.

2.2. Catalyst characterization

Catalysts chemical composition was determined by ICP analysis.

The crystallinity of as prepared samples, and after catalytic tests, was evaluated by XRD, in a Rigaku diffractometer with an incident Cu Kα radiation.

H_2-TPR (temperature programmed reduction) experiments were performed using samples of 130 mg of catalyst (dry base), heated from room temperature (RT) to 1000 °C at 7.5 °C min^{-1}, under a mixture of H_2/Ar (5%) with a flow rate of 1.5 L h^{-1}. Hydrogen consumption was measured with a TCD (thermal conductivity detector); water was trapped in a dry ice-cooled trap; TCD calibration, with a mixture of H_2 (5 vol.%)/He, was performed prior to each experiment.

DRS (diffuse reflectance) UV–vis spectra were obtained in a UV spectrometer Shimadzu MPC 3100 equipped with a diffuse reflectance attachment that possesses an integrating sphere coated with $BaSO_4$. Spectra were recorded at a medium speed, with a slit width 5 nm and a sampling interval equal to. The absorption intensity was calculated from Kubelka–Munk theory where $F(R_\infty)$ is proportional to the absorption coefficient. All samples were dehydrated before the analysis and kept under vacuum atmosphere until the analysis was completed, in order to avoid Co ions to coordinate with water molecules [10].

Temperature programmed desorption (TPD) of NO was conducted in the same reactor system used for catalytic tests (described below). For a typical TPD measurement, 0.170 mg of sample was used. The sample was pre-treated in flowing He from RT to 500 °C with a heating rate of 5 °C min^{-1} and kept at 500 °C for 1 h. The sample was then cooled to RT under He flow. The adsorption of NO was carried out during 90 min at room temperature with a mixture of NO (1000 ppm) in He with a total flow of 250 cm^3 min^{-1}. The sample was then flushed with He at room temperature to eliminate gaseous and weakly adsorbed NO, recovering the initial base line. NO TPD was then carried out under He flow (or with a mixture of CH_4 – 2000 ppm – and He), from room temperature to 500 °C at a heating rate of 10 °C min^{-1}. The products were monitored simultaneously by a Balzers mass spectrometer (Prisma QMS200) and a chemiluminiscence detector (Thermo Electron Co. 42C, NO–NO_2–NO_x high level analyzer). The products were

registered continuously as a function of time and temperature by mass spectrometer (*m/e* = 28, 30, 32, 44 and 46).

Temperature programmed surface reaction (TPSR) was performed with the same apparatus used for NO-TPD. Catalysts were pre-treated in He and, after catalysts reached the room temperature, they were submitted to the usual gas mixture used with the catalytic tests. TPSR experiments were carried out with a heating rate of 10 °C min^{-1}. Reaction products were analysed by chemiluminiscence and by a mass spectrometer (*m/e* = 15, 18, 28, 30, 32, 44 and 46) as a function of time and temperature.

2.3. Steady-state reduction of NO by methane

The reduction of NO by methane in the presence of oxygen excess was carried out in a fixed-bed flow reactor, typically with 170 mg of the catalyst. A gas mixture containing 1000 ppm NO, 2000 ppm CH_4, 5 vol.% O_2, 2 vol.% H_2O and He for balance was feed at a rate of 250 cm^3 min^{-1}, through mass flow controllers (Brooks 5850). The corresponding GHSV was 45,000 h^{-1}, considering a bulk catalyst density of 0.5 g cm^{-3}. Catalysts were pre-treated under He at 500 °C with a heating rate of 5 °C min^{-1} for 1 h, prior to reaction. Then catalysts were cooled to reaction temperature and kept in contact with the gas mixture for 1 h before the first analysis, in order to reach the steady state. Catalytic tests were then carried out for 2 h for each temperature, in a range between 350 and 550 °C. Feed and effluent gases compositions were analysed by using an on-line gas chromatograph (HP 5890 Series II) with two columns, MolSieve 5A and Poraplot Q, and two detectors in series: TCD detector used to analyse N_2, O_2, CO_2 and CO and FID detector used to analyse CH_4. When the reaction was carried out in wet conditions (2% H_2O), the mixture passes through an ice-cooled trap, prior to chromatograph, in order to remove most of the water contained in the gas stream.

Catalytic tests occurred in the following sequence: (1) a run under dry conditions, from 350 to 550 °C – 1st dry cycle; (2) a run under wet conditions (2 vol.% H_2O), from 400 to 550 °C – 2% water; (3) a run in dry conditions after the suppression of water from gas stream, from 350 to 550 °C – 2nd dry cycle.

Formation of nitrogen was used to calculate NO conversion and methane conversion was obtained by following the change in the methane peak area.

3. Results and discussion

The distinct methods used for the preparation of catalysts lead to two samples apparently very analogous. The chemical composition as well as Co/Al and Pd/Al are presented in Table 1. Cobalt and palladium loadings are very similar in both samples.

X-ray diffraction also showed that both samples preserved their crystallinity after metal loading, thermal treatment and catalytic tests.

However, the order of introduction of Co and Pd cations seems to have a significant influence in the catalytic behaviour both in dry and wet conditions. Differences in the amount, distribution and type of species present in each catalyst were also observed. An attempt to understand these differences and its relation with the catalytic behaviour will be made with the present discussion.

Table 1
Chemical composition of prepared catalysts

Catalyst	Co (wt.%)	Pd (wt.%)	Co/Al	Pd/Al
PdCo-HFER	2.2	0.15	0.23	0.01
CoPd-HFER	2.0	0.16	0.21	0.01

3.1. Steady-state reduction of NO by methane

PdCo-HFER and CoPd-HFER catalysts were tested in the selective catalytic reduction of NO with methane in the presence of oxygen excess under dry and wet conditions. Fig. 1 exhibits the evolution of NO conversion into N_2 as a function of temperature and Fig. 2 respects to the total oxidation of methane. Both in dry and wet conditions, PdCo-HFER (Co introduced prior to Pd) have a better performance for NO reduction in all temperature range. The conversion of NO into N_2 reached by PdCo-HFER is considerably higher than for CoPd-HFER, especially at lower temperatures: at 450 °C PdCo-HFER catalyst presents a conversion of 44% and CoPd-HFER only 26%. Both catalysts exhibit a loss of activity under wet conditions: at 450 °C, PdCo-HFER drops the conversion to 27% (about 40% decrease) and CoPd-HFER to 11% (about 60% reduce). Even though, after the removal of water from the gas stream, both catalysts recover the initial activity (results not shown), strongly suggesting that, under test conditions, the loss of activity might be related only with a competitive adsorption.

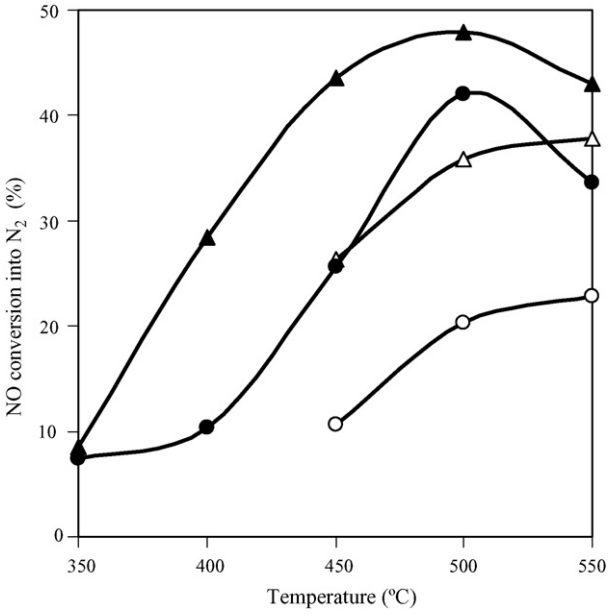

Fig. 1. Conversion of NO into N_2 for PdCo-HFER (▲) and CoPd-HFER (●). Full symbols for dry conditions and open symbols for wet conditions. NO, 1000 ppm; CH_4, 2000 ppm; O_2, 5%; H_2O 2 vol.%; GHSV = 45,000 h^{-1}.

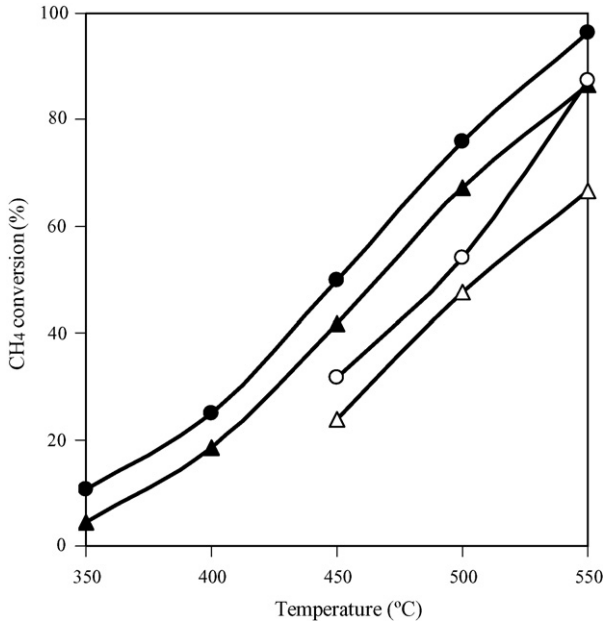

Fig. 2. Total CH_4 conversion for PdCo-HFER (▲) and CoPd-HFER (●). Full symbols for dry conditions and open symbols for wet conditions. NO, 1000 ppm; CH_4, 2000 ppm; O_2, 5%; H_2O 2 vol.%; GHSV = 45,000 h^{-1}.

For the total methane oxidation, CoPd-HFER shows a better catalytic performance in all temperature range both in dry and wet conditions.

3.2. Co^{2+} and Pd^{2+} location in the zeolite structure

The distribution of metal species in the zeolite structure is an important feature to evaluate the differences resulting from the preparation method.

The analysis of UV–vis spectra allows to evaluate the presence of bare Co^{2+} ions and their relative distribution among the different cationic zeolite exchange sites and to verify how the order of introduction of the metal cations affects this distribution. Fig. 3 illustrates the spectra of dehydrated CoPd-HFER and PdCo-HFER samples both evidencing the bands characteristics for the d–d transitions of the Co^{2+} ions in the range 14,000–22,000 cm^{-1}. Both spectra evidence the presence of two broad bands, one between 16,000 and 18,000 cm^{-1} and the other at about 21,000 cm^{-1}. The deconvolution of the obtained spectra for PdCo-HFER and CoPd-HFER into Gaussian bands can be performed according to the literature [10], in order to identify the three different spectral components normally attributed to the three different locations of Co cations at α, β and γ sites. The single band with a maximum at 15,000 cm^{-1} corresponds to component α. Component β is decomposed into four bands at 16,000, 17,100, 18,700 and

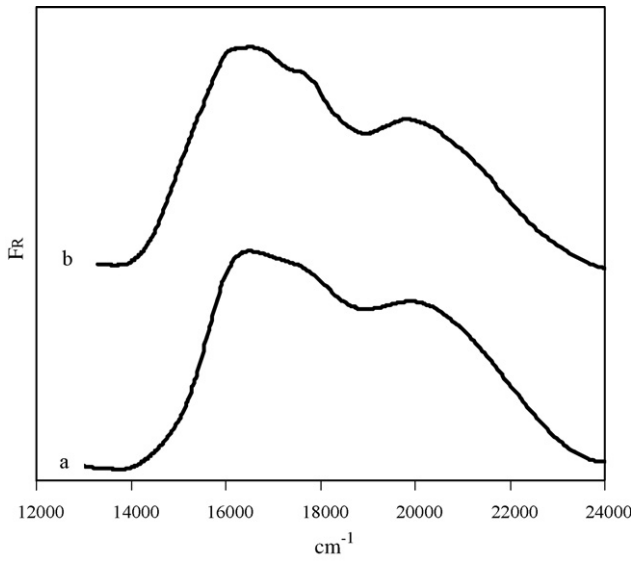

Fig. 3. Normalized visible spectra of fresh samples: (a) PdCo-HFER and (b) CoPd-HFER.

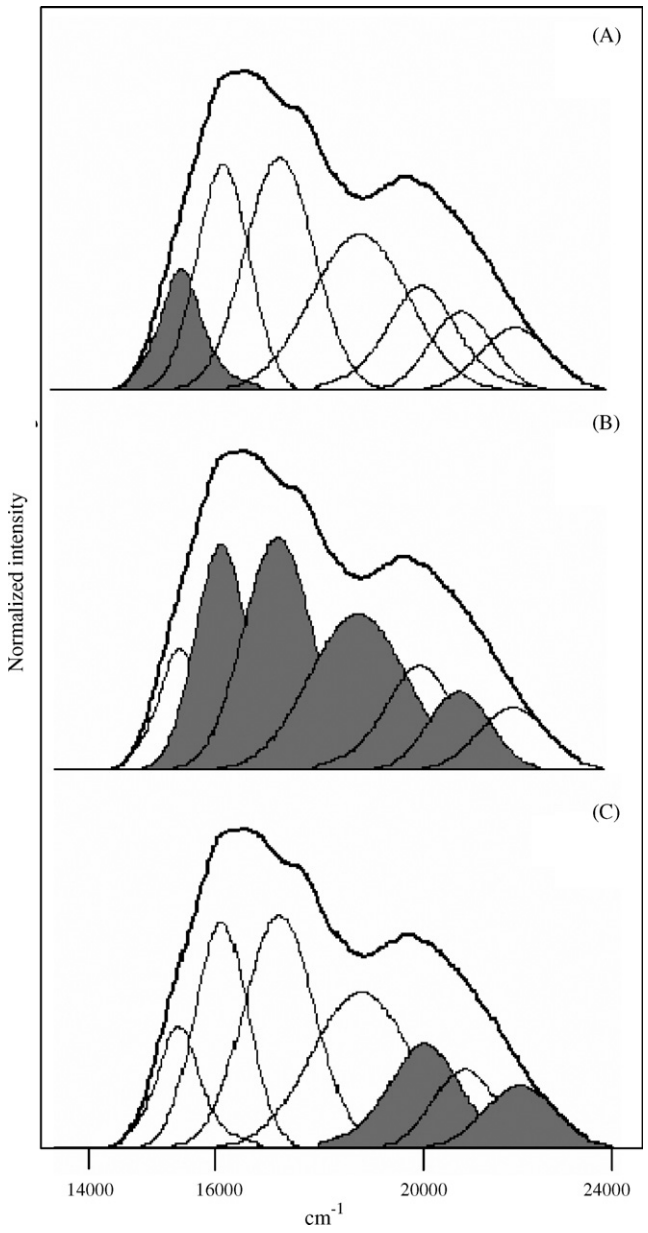

Fig. 4. Decomposition of the visible spectra of CoPd-HFER to Gaussian curves: (A) component α indicated by a shadow area, (B) component β indicated by a shadow area and (C) component γ indicated by a shadow area.

20,600 cm^{-1}. The γ component is decomposed into two bands at 20,300 and 22,000 cm^{-1}. Fig. 4 exhibits the deconvolution spectra for CoPd-HFER into the Gaussian bands.

The band at lower wave numbers (15,000 cm^{-1}) has a higher relative intensity for CoPd-HFER sample. This fact clearly put in evidence that CoPd-HFER has more Co^{2+} ions in α position than PdCo-HFER. The relative distribution of Co^{2+} ions for the available sites α, β and γ is presented in Table 2. The obtained results reveal that for both samples β sites are the most populated and that there is a significant difference between the catalysts in what α and γ population concerns. CoPd-HFER catalyst (Pd introduced prior to Co) exhibits 10 times more Co^{2+} in α position (wall of main channels) than PdCo-HFER. As previously reported [10], the introduction of others cations, namely Cs and Ba, prior to cobalt, significantly affect the spectrum of Co-HFER: the presence of these cations increases the relative intensity of the absorption band at 15,000 cm^{-1}. When Co is introduced prior to Pd (PdCo-HFER catalyst), and during the first calcination procedure, Co ions can migrate or be stabilised in more favourable positions (β and γ), which are not left even after Pd ion-exchange procedure, as no significant differences in UV–vis spectra of Co-HFER (spectrum not shown) and PdCo-HFER were observed. In this case only a slight decrease in α population after the introduction of Pd is detected. This fact has already been reported for other structures containing both Co and Pd [7]. On the contrary, for CoPd-HFER catalyst, in which Pd was introduced prior to Co, a different distribution in the relative population of Co ions can be detected. It had already been reported, for MOR structure [7], that Pd^{2+} is primarily stabilised in β sites. The results obtained in the present work seem to indicate that Pd^{2+} prefers to be located in γ sites in FER structure and Co will tend to occupy the α positions on the main channels. Due to the low content of Pd (0.15%) it is probable that in the case of the CoPd-HFER catalyst, all Pd ions are located in β and γ sites and the probability to find Pd in the main channels is much reduced. However, the introduction of Pd after Co (PdCo-HFER catalyst) can lead to a catalyst with some Pd ions in the main channels of FER and consequently, closer to Co ions previously located in α positions.

3.3. Reducibility and identification of different Co and Pd species

H_2-TPR and XPS analysis were performed in order to detect the presence of different metal species arising from the different preparation methods. H_2-TPR can distinguish different species with different reduction temperatures and according with those temperatures an approach to the type and location of these species in the zeolite framework will be attempted. XPS analysis will be used to analyse metals distribution in the outer surface of zeolite particles.

Table 2
Relative distribution in α, β and γ sites of Co^{2+} cations

Catalyst	α	β	γ
PdCo-HFER	1	71	28
CoPd-HFER	10	71	19

The H_2-TPR profiles for both catalysts are exhibited in Fig. 5. In both profiles several reduction processes can be detected between 150 and 800 °C that have been assigned to different types of cobalt species: (i) between 150 and 300 °C, the reduction processes are normally assigned to cobalt oxide species that interact with zeolite protons, Co-oxo ions [17,18]; (ii) the process with a maxima around 400 °C corresponds to the reduction of Co_3O_4 species [4,17,19,20] that is consistent with previous results obtained for a mechanical mixture Co_3O_4/HFER that showed a peak at 350 °C (not presented); (iii) species that reduce between 500 °C [17] and 800 °C [4] had been ascribed, in other structures, to cobalt oxide species inside the pores of the zeolite, so more difficult to reduce [21]. Finally, at higher temperatures (>800 °C), the reduction of Co^{2+} ions located in exchanged positions is detected [17].

An attempt to quantify H_2 consumption was made. The total consumption of hydrogen is very similar in both samples. In both catalysts the hydrogen consumption involved in the different reduction processes is quite low. This fact has already been reported [4,22] and the lack between the expected ratio and the obtained one has been attributed to the fact that part of cobalt species might be located in inaccessible positions [17,21,23].

Reduction of palladium species is observed at temperatures around 100 °C, corresponding to a sharp peak. This process is observed in both catalysts but with a relevant difference: PdCo-HFER did not exhibit a lonely and well defined peak but instead of that it shows a peak with a shoulder at lower temperature and a continuous reduction process that overlaps with the process normally attributed to the reduction of oxo-cations. To explain this we consider first the reduction of bimetallic/multimetallic species of Co and Pd and eventually the presence of cobalt oxides much easier to reduce, like very small oxide crystals or located in the vicinity of palladium [24]. On the other hand the presence of oxo-cations (peak at 230 °C) is only detected for PdCo-HFER catalyst.

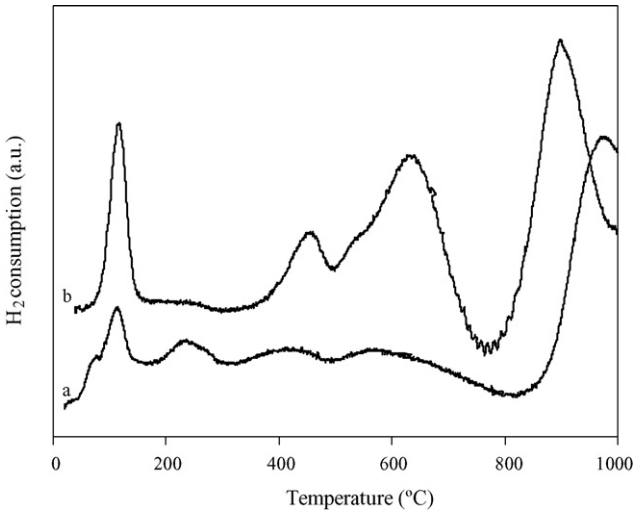

Fig. 5. H_2-TPR profiles of (a) PdCo-HFER and (b) CoPd-HFER.

Both catalysts exhibit the presence of Co_3O_4 and cobalt oxide species located inside the pores of zeolite. The reduction processes of these species its better defined in CoPd-HFER with maxima at 460 and 640 °C and the H_2 consumption is twice that those presented by PdCo-HFER for the reduction processes at about 600 °C.

Concerning the reduction peaks of Co^{2+} ions in exchange positions (>800 °C), it can be observed that there is a difference of about 80 °C in the maximum of the peaks: Co^{2+} ions are more easily reduced in CoPd-HFER catalyst. In fact, the UV–vis spectrum of this catalyst has evidenced a higher content of Co^{2+} located in more accessible positions of main channel (α sites). It is probable that the reduction of Co^{2+} ions located in sites β and γ should be energetically more demanding than the reduction of the Co^{2+} ions placed in the more accessible α sites. Consequently, the increase in the reduction temperature of Co^{2+} ions, observed for PdCo-HFER catalyst, can be attributed to the fact that this catalyst revealed a lower content in cobalt ions located in α positions or to a less efficient activation of H_2 by the Pd species present in this sample.

Furthermore, XPS analysis of these catalysts revealed that CoPd-HFER catalyst presents a higher amount of Co in the outer surface of the catalyst particles, while no Pd was detected in the surface. For PdCo-HFER both Co and Pd were detected at the surface of the zeolite. Both UV–vis and XPS analysis seem to be in good agreement with the obtained TPR profiles and the above interpretation.

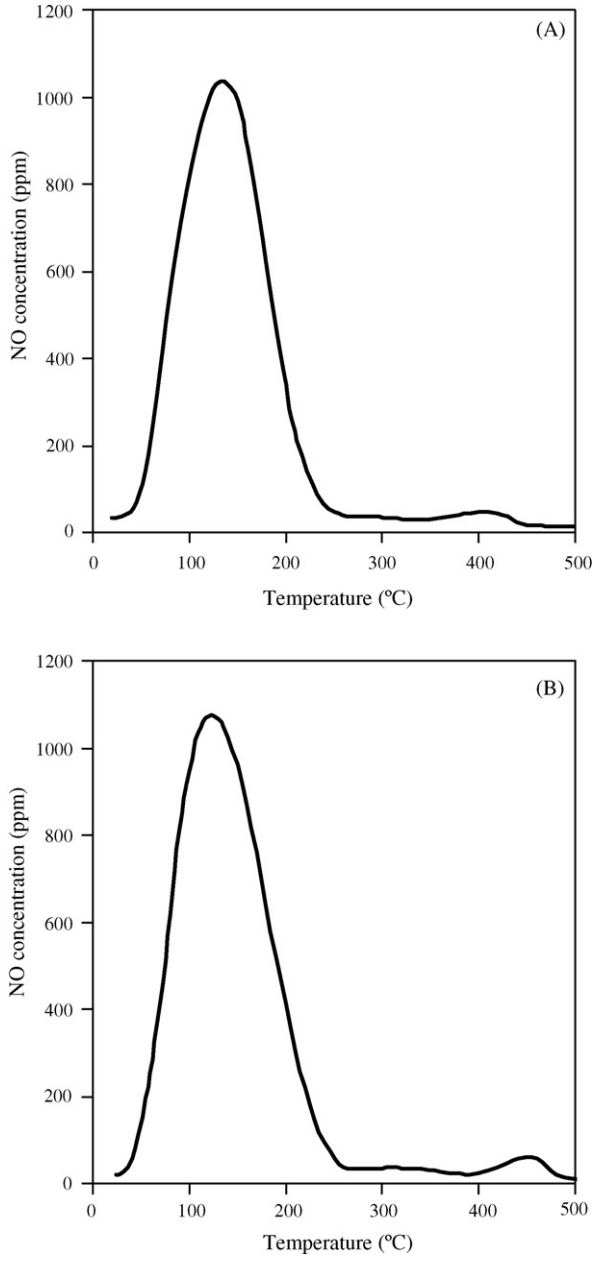

Fig. 6. NO TPD for PdCo-HFER (A) and CoPd-HFER (B). Adsorption conditions: 1000 ppm NO in He, RT. Desorption under He.

3.4. TPD of NO

NO-TPD analysis has been extensively studied with several zeolite based catalysts, ion-exchanged with Co and Pd [25–28]. Results of TPD of NO are shown in Fig. 6A and B, for PdCo-HFER and CoPd-HFER, respectively. During the adsorption of NO at room temperature both catalysts exhibit N_2O release, what means that the metallic species present in these catalysts are able to promote the disproportionation of NO into N_2O ($3NO \rightarrow N_2O + NO_2$); the fact that no NO_2 release is observed means that it had remain adsorbed. This type of results was previously reported to occur on reduced Pt catalysts [27], and the role of N_2O species in lean deNO_x process has been largely discussed [29].

TPD profiles shown in Fig. 6A and B are very similar. For the first peak of desorption, the intensity and temperature of maxima are the same for both catalysts. However, at higher temperatures, some differences can be detected. A magnification of TPD profiles on this range of temperatures can be observed in Fig. 7, which shows that CoPd-HFER exhibits two desorption peaks with maxima at 350 and 450 °C and PdCo-HFER exhibits a

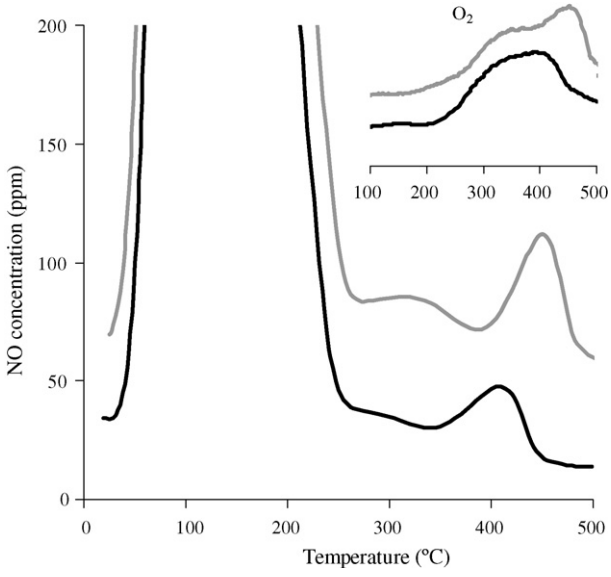

Fig. 7. NO TPD for PdCo-HFER (black) and CoPd-HFER (grey).

shoulder at the end of the first desorption peak and a peak at 410 °C. These high temperature desorption peaks can be related with the decomposition of nitrate species formed at lower temperatures since simultaneously the release of oxygen can be observed. No N_2 release was detected which indicates that no decomposition of NO into N_2 and O_2 occurs in the studied catalysts from RT to 500 °C.

During these TPD experiments, release of NO_2 and N_2O was also registered, probably originated from disproportionation of NO (Fig. 8A and B). PdCo-HFER releases NO_2 between 100 and 450 °C and lower temperatures desorption are much more significant than in CoPd-HFER. For temperatures above 300 °C, CoPd-HFER exhibits a very significant desorption of NO_2. It appears that with this catalyst, NO_2 is strongly adsorbed. Desorption of N_2O occurs at higher temperatures for PdCo-HFER and at lower temperatures for CoPd-HFER catalyst.

The adsorption/desorption of NO seems to be related with: (i) the capacity of each catalyst to adsorb more strongly NO and NO_2 species on its surface; (ii) the ability to form and release NO_2 and N_2O. From the above results, become visible that the main particularities observed on these two catalysts are related with the formation of NO_2 and the capacity of the catalyst to retain it adsorbed on its surface. CoPd-HFER that had required higher temperatures to decompose nitrate species (Fig. 7), also evidenced a stronger capacity to retain NO_2 adsorbed on its surface. PdCo-HFER seems to have an increased capacity to originate NO_2, which is less strongly adsorbed on the surface of the catalyst.

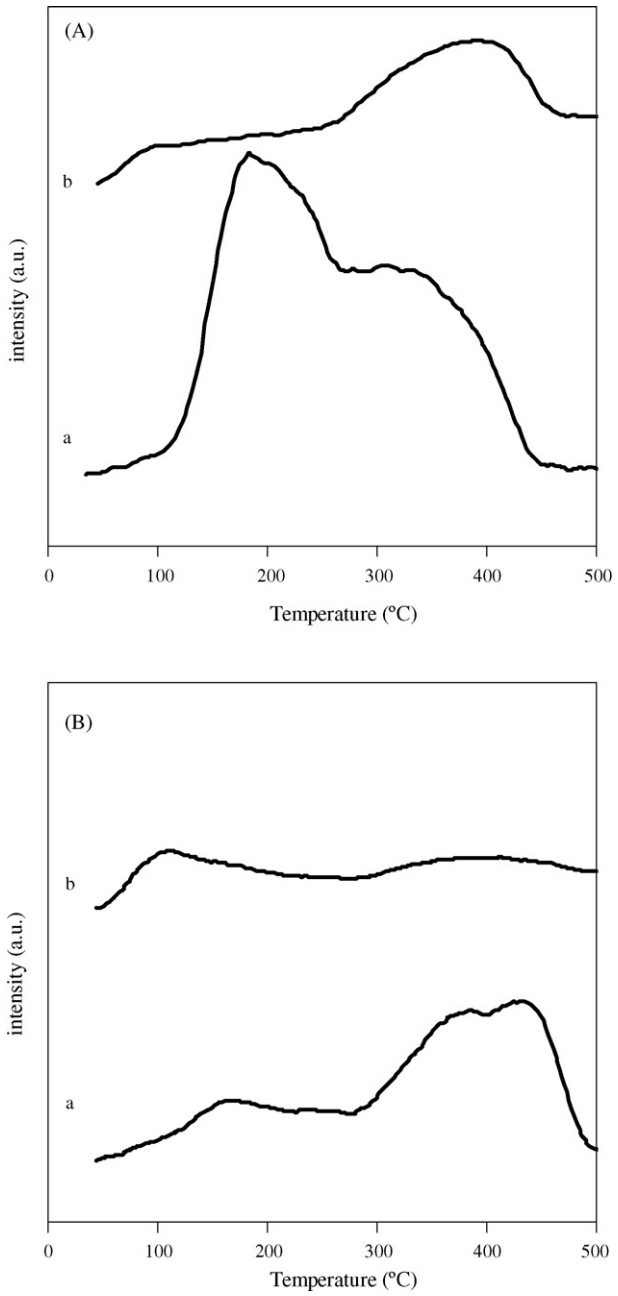

Fig. 8. NO TPD for PdCo-HFER (A) and CoPd-HFER (B). Curves (a) for NO_2 desorption and curves (b) for N_2O desorption. Adsorption conditions: 1000 ppm NO in He, RT. Desorption under He.

3.5. TPSR of NO and NO_2

The NO desorption studies reveal significant differences between the catalysts in what NO_2 formation and desorption is

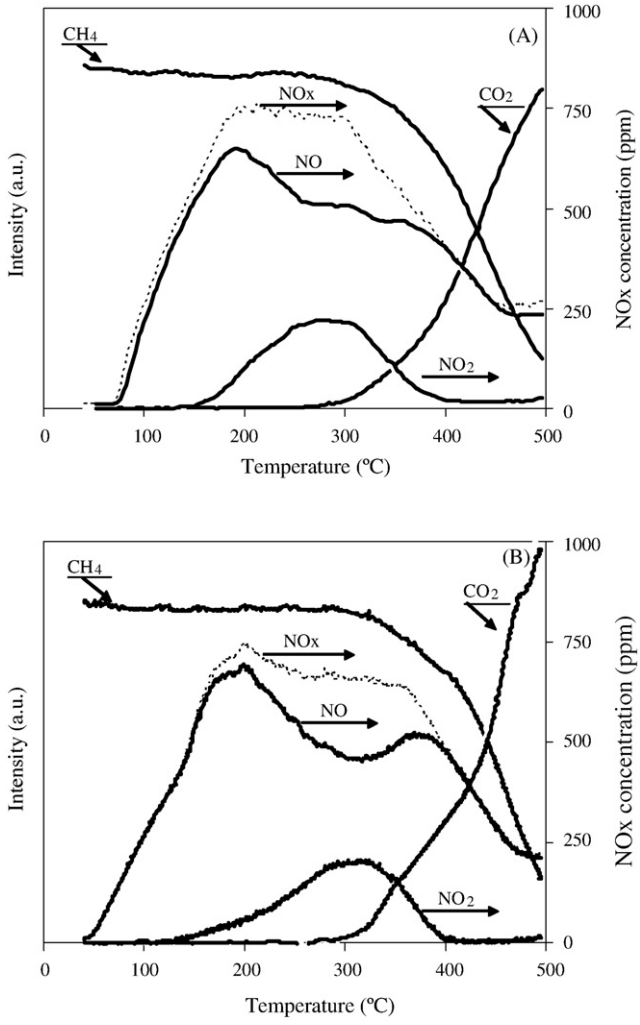

Fig. 9. TPSR for PdCo-HFER (A) and CoPd-HFER (B). NO, 1000 ppm; CH_4, 2000 ppm; O_2, 5%; He.

concerned. To understand this fact and the importance of NO_2 in the mechanism of NO reaction with CH_4 and O_2, two different TPSR experiments were performed one in the presence of NO and another in the presence of NO_2. The main goal is to put in evidence the role of NO_2 as a reaction intermediate with major significance.

Temperature programmed surface reaction of NO with methane in the presence of oxygen excess is shown in Fig. 9A and B. The evolution of CH_4 and CO_2 is similar in both catalysts. There is a difference concerning the temperature of methane activation and CO_2 release; these phenomena start about 40 °C earlier in PdCo-HFER catalyst. For NO_x species, studied catalysts also exhibit a different behaviour. The amount of NO_2 released from PdCo-HFER is higher than from CoPd-HFER, namely at lower temperatures; between 180 and 300 °C, NO consumption results in NO_2 formation since NO_x remains constant. For CoPd-HFER (Fig. 9B) NO_x decreases between 200 and 260 °C probably due to: (i) the production of NO_2 which is not immediately released because this catalyst has a strong tendency to retain these adsorbed species (Fig. 8B); (ii) the fact that NO_2 is being used for the production of R–NO_x species [28]. In PdCo-HFER catalyst NO_x rapidly decrease for

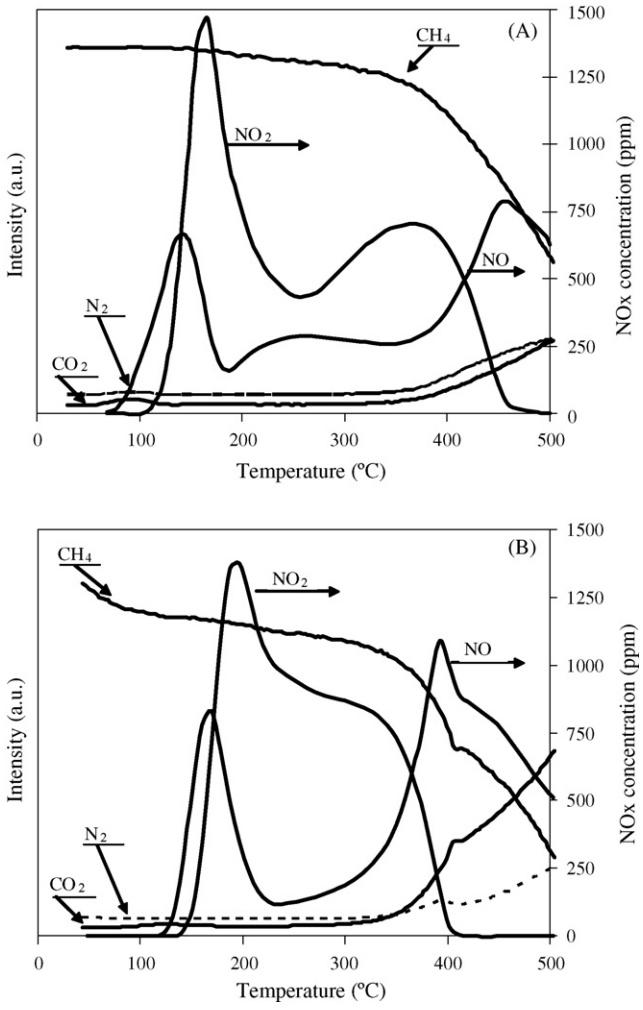

Fig. 10. TPSR for PdCo-HFER (A) and CoPd-HFER (B). NO_2, 1000 ppm; CH_4, 2000 ppm; O_2, 5%; He.

temperatures above 300 °C, while with CoPd-HFER this phenomenon is only observed at 375 °C. Furthermore, an increase of NO release between 300 and 400 °C can be detected with CoPd-HFER, which can be explained by some ability of this catalyst to entrap NO_x species which are liberated only with increasing temperature. For temperatures higher than 400 °C the behaviour is similar to the observed for PdCo-HFER.

TPSR of NO_2 with methane in the presence of oxygen excess was carried out for both catalysts and is reported in Fig. 10A and B. For these TPSR measurements we observe a complete different behaviour in a general way. The behaviour of the catalysts in what methane concerns is completely different: for PdCo-HFER: the evolution of CH_4 is practically constant and its consumption goes together with the release of CO_2 which starts at 350 °C. At low temperature (about 100 °C) a small peak for mass 44 was detected, but in this case it is attributed to N_2O instead of CO_2 (see curve identified as CO_2), because no consumption of CH_4 is observed. In the case of CoPd-HFER catalyst (Fig. 10B) a slight decrease of CH_4 is observed until the temperature of 300 °C is reached. At temperatures higher than 300 °C, CH_4 consumption goes together with the release of CO_2. Around 400 °C we verify the occurrence of small peaks (negative for CH_4 and positive for CO_2 and N_2), that evidence the simultaneous effect of the fast consumption of CH_4, the formation of CO_2 and N_2 and release of NO, the last one with a very intense peak. This can be explained by the formation, storage and decomposition of intermediate R–NO_x species, according to the reaction mechanisms already proposed by Djéga-Mariadassou [28] and references there in. This behaviour was not observed for PdCo-HFER.

PdCo-HFER catalyst exhibit a first NO_2 peak with maximum at about 170 and at 400 °C it still continues desorbing NO_2, contrarily to the other catalyst that shows the first peak at about 200 and at 400 °C the NO_2 release is practically zero. For temperatures above 200 °C the direct conversion of NO_2 to NO controlled by thermodynamic equilibrium [27] starts and simultaneously we can observe an increase of NO. On the other hand the observed evolution of N_2 indicates that deNO_x reaction starts at 300 °C for PdCo-HFER and at 350 °C for CoPd-HFER catalyst. The release of NO_x in this temperature range is significantly higher for CoPd-HFER, which means that this catalyst exhibits a lower conversion into N_2. These observations are also in agreement with the results observed for catalytic tests of NO reduction performed in steady state (Fig. 1).

These results show once more that the two studied catalysts have different catalytic behaviours, and the differences can be exalted using NO_2 as reactant. It appears that active sites present in each one of the catalysts and their location have a major importance for the catalytic behaviour. The differences between the metallic active sites previously reported and their role in the formation of NO_2 and subsequent intervention on the lean deNO_x process with CH_4 are well visible.

3.6. An approach to CH_4-SCR mechanism

Several approaches to the mechanism had already been made [28–32] and the reaction pathways always involve the

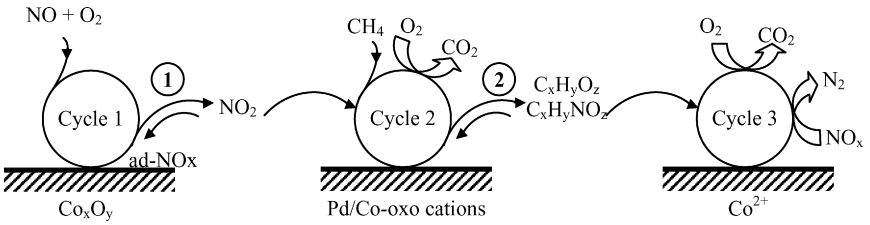

Fig. 11. Scheme for the reaction mechanism for the selective reduction of NO by methane in the presence of oxygen.

formation of organic species like R–NO_x, R–NO, R–ONO, R–NO_2, R–ONO_2 and CxHyOz. However the active sites for the formation of these species still remain under discussion. Some authors [6,28,33] reported the formation of NO_2 on Co_3O_4 species. Other authors [4,17] believe that NO_2 formation can occur also on other type of cobalt oxides, like Co-oxo cations, but the kind of cobalt oxides and their location has not been yet clarified. Both the studied catalysts exhibit the presence of these species but their amount and location are quite different, as well as the adsorption energy between active sites and NO_2. Another relevant issue concerns the proximity between metallic sites: while for PdCo-HFER it seems that there is some closeness between the different metallic species, for CoPd-HFER this is not so clear. The lack of Pd species in the surface of this catalyst, showed by XPS, confirms that at least no Pd species exist near the cobalt oxides species present in the outer surface of the catalyst.

The consequences of these features in the catalytic behaviour of both catalysts can be interpreted in terms of reaction mechanism. According to the mechanism proposed by Djéga-Mariadassou [28] there are three cycles, schematically exposed in Fig. 11.

CoPd-HFER catalyst seems to retain NO_2 more strongly adsorbed than PdCo-HFER. If so, there is less NO_2 available to participate in cycle number 2. Another relevant fact is that CoPd-HFER exhibits lower selectivity for N_2 than PdCo-HFER. It means that oxygen competes with NO_2 as an oxidant, leading to selectivity decrease. The observed storage of R–NO_x compounds during the TPSR measurements performed on CoPd-HFER catalyst lead to a smaller amount of intermediate compounds available to the third cycle. On PdCo-HFER, there is no evidence of retention of NO_2 neither R–NO_x compounds, which means that steps 1 and 2 are faster and deNO_x catalysis is favoured. The main differences detected in the catalytic sites present in both catalysts concern the quantity of cobalt oxides, the existence of Co-oxo cations, and an eventual direct interaction of cobalt and palladium species, which are detected only in PdCo-HFER. The high quantity of cobalt oxides detected by TPR of H_2 on CoPd-HFER, can be responsible by the formation and retention of NO_2, which means that these oxidic species influence the first step of the reaction. In the case of PdCo-HFER catalyst, the balance between the several cobalt species seems to be more satisfactory; in addition, this catalyst possess Co-oxo cations and probably an improved interaction between Pd and Co species, both presumed to be involved in step 2. Moreover, it appears that the observed proximity between the different metal species, at least at the outer surface of the catalyst, can improve the catalytic behaviour, probably increasing steps 1 and 2 rates.

Finally, the differences observed in the distribution and reducibility of Co^{2+} ions, which are involved mainly in step 3 seem to have a minor effect relatively to the other metal species involved into the two first cycles.

4. Conclusions

The present work shows that the preparation of bimetallic cobalt/palladium-based FER catalysts should be optimized in order to attain a good balance between all actives sites involved in CH_4-SCR reaction. The simple change in the order of addition of metals to catalyst, gives rise to totally diverse species both in type and quantity but also in location within zeolite framework.

It is very important to have cobalt and palladium species able to push the key reaction intermediate (NO_2) among the main cycles of the reaction mechanism. An exaggerated retention of NO_2, eventually under the form of R–NO_x intermediates, must be avoided in order to assist the subsequent mechanistic pathways.

The proximity between Co and Pd species improves the global catalytic behaviour, and Co-oxo cations together with palladium species have a major role as catalytic active sites for the activation of methane. Furthermore, the large amount of cobalt oxides can be in the origin of an excessive retention of adsorbed NO_2, which is not enough available to activate methane and consequently the reaction rate decreases.

Acknowledgements

The authors thank Professor Djéga-Mariadassou for fruitful discussions. We thank Dr. Ana Rego for kindly having performed XPS measurements and by valuable discussions. Financial support from FCT (Fundação para a Ciência e Tecnologia) is gratefully acknowledged.

References

[1] M. Iwamoto, H. Hamada, Catal. Today 10 (1991) 57.
[2] Y. Li, J.N. Armor, Appl. Catal. B 1 (1992) L31.
[3] F. Bustamante, F. Córdoba, M. Yates, C. Montes de Correa, Appl. Catal. A 234 (2002) 127.
[4] J.A.Z. Pieterse, R.W. van den Brink, S. Booneveld, F.A. de Bruijn, Appl. Catal. B 39 (2002) 167.
[5] K. Kagawa, Y. Ichikawa, S. Iwamoto, T. Inui, Catal. Lett. 52 (1998) 145.

[6] T.J. Lee, I.-S. Nam, S.W. Ham, Y.S. Baek, K.H. Shin, Appl. Catal. B 41 (2003) 115.
[7] M. Ogura, S. Kage, T. Shimojo, J. Oba, M. Hayashi, M. Matsukata, E. Kikuchi, J. Catal. 211 (2002) 75.
[8] H. Christian, Le L. Olivier, M. Nadege, S.J. Jacques, US Patent 6,063,351, 2000. Gaz de France.
[9] B. Wen, W.M.H. Sachtler, Catal. Lett. 86 (2003) 39.
[10] D. Kaucký, J. Dědeček, B. Wichterlová, Micropor. Mesopor. Mater. 31 (1999) 75.
[11] Z. Sobalík, J. Dědeček, D. Kaucký, B. Wichterlová, L. Drozdová, R. Prins, J. Catal. 194 (2000) 330.
[12] B. Wichterlová, Top. Catal. 28 (2004) 131.
[13] G. Djéga-Mariadassou, M. Boudart, J. Catal. 216 (2003) 89.
[14] R.H.H. Smits, Y. Iwasawa, Appl. Catal. B 6 (1995) L201.
[15] M. Misono, CATTECH 2 (1998) 183.
[16] E.A. Lombardo, G.A. Sill, J.L. d'Itri, W.K. Hall, J. Catal. 173 (1998) 440.
[17] X. Wang, H. Chen, W.M.H. Sachtler, Appl. Catal. B 26 (2000) L227.
[18] L.F. Córdoba, G.A. Fuentes, C.M. de Correa, Micropor. Mesopor. Mater. 77 (2005) 193.
[19] J.A.Z. Pieterse, R.W. van den Brink, S. Booneveld, F.A. de Bruijn, Appl. Catal. B 46 (2003) 239.
[20] X. Wang, H. Chen, W.M.H. Sachtler, Appl. Catal. B 29 (2001) 47.
[21] L.B. Gutierrez, A.V. Boix, E.A. Lombardo, J.L.G. Fierro, J. Catal. 199 (2001) 60.
[22] J. Dědeček, L. Căpek, D. Kaucký, Z. Sobalík, B. Wichterlová, J. Catal. 211 (2002) 198.
[23] Z. Sobalík, J. Dědeček, I. Ikonnikov, B. Wichterlová, Micropor. Mesopor. Mater. 21 (1998) 525.
[24] A.P. Ferreira, C. Henriques, M.F. Ribeiro, F.R. Ribeiro, Catal. Today 107/108 (2005) 181.
[25] M. Ogura, M. Hayashi, S. Kage, M. Matsukata, E. Kikuchi, Appl. Catal. B 23 (1999) 247.
[26] Y. Li, J.N. Armor, J. Catal. 150 (1994) 376.
[27] R. Marques, P. Darcy, P. Da Costa, H. Mellottée, J.M. Trichard, G. Djéga-Mariadassou, J. Mol. Catal. A 221 (2004) 127.
[28] G. Djéga-Mariadassou, Catal. Today 90 (2004) 27.
[29] R. Burch, J.P. Breen, F.C. Meunier, Appl. Catal. B 39 (2002) 283.
[30] A.D. Cowan, R. Dumpelmann, N.W. Cant, J. Catal. 151 (1995) 356.
[31] M. Ogura, Y. Sugiura, M. Hayashi, E. Kikuchi, Catal. Lett. 42 (1996) 185.
[32] A.W. Aylor, L.J. Lobree, J.A. Reimer, A.T. Bell, Stud. Surf. Sci. Catal. 101 (1996) 661.
[33] M. Haneda, Y. Kintaichi, H. Hamada, Appl. Catal. B 55 (2005) 169.